New Approaches for Synthesizing γIII-CoOOH by Soft Chemistry

F. Bardé,*,† M.-R. Palacin,‡ B. Beaudoin,† A. Delahaye-Vidal,† and J.-M. Tarascon†

Laboratoire de Réactivité et Chimie des Solides (LRCS), UMR 6007 CNRS, Université de Picardie Jules Verne, 33 rue Saint Leu, Amiens, France, and Institut de la Ciència de Materials de Barcelona (CSIC), Campus UAB, 08193 Bellaterra, Catalunya, Spain

Received April 2, 2003. Revised Manuscript Received November 5, 2003

Two soft chemical processes enabling the low-temperature synthesis of γIII-CoOOH are reported. Both processes consist of an oxidation reaction of αII-$Co(OH)_2$ performed either in dry conditions (ozonation) or in solution. The γIII-CoOOH phase is usually prepared using a ceramic step process, which hinders its synthesis as a coating to improve the electrochemical performance of the active nickel hydroxide positive electrode in Ni-based batteries. Through this work, new γIII-CoOOH phases presenting properties quite different from those of the ceramic γIII-COOOH are obtained. The chemical stability in concentrated potassium hydroxide solution and the electrochemical behavior of these new phases have also been studied.

Introduction

The beneficial effect of cobalt additives on the positive electrode of Ni/Cd or Ni/MH batteries was clearly demonstrated in numerous former studies.[1−4] Most nickel electrodes are fabricated with cobalt-doped hydroxides or contain cobalted phases as additives. There have been recent studies[5,6] on the redox mechanisms of the cobalt hydroxides in KOH media. Cobalt (II) hydroxide can be oxidized to yield several phases, such as stoichiometric βIII-CoOOH or nonstoichiometric β′III-CoOOH and γIII-CoOOH. The latter contain Co^{4+} cations that are claimed to be critical for electrode conductivity enhancement.

Battery manufacturers have long experienced the positive attributes of such an added phase to the nickel oxihydroxide electrode (NOE) in enhancing its electrochemical performance, namely limiting its self-discharge and increasing its capacity and conductivity. These beneficial effects of cobalted additives, especially avoiding self-discharge, might be optimized when they are not simply added to the nickel hydroxide active materials and well mixed, but form a coating around the nickel hydroxide particles.[1−7] This has been reported for β-CoOOH phases, but never for γ-CoOOH, because the only known synthetic route to the latter involves a ceramic step, and this is not compatible with the thermal stability of $Ni(OH)_2$. In that context, we pursued different routes aiming toward the oxidation of cobalt hydroxides, being well aware that we had to limit ourselves to the soft chemistry process for chemical/thermal stability reasons.

Many investigations have been devoted to the synthesis of oxidized cobalt phases. Among them are (1) oxidation of βII-$Co(OH)_2$ by means of sodium hypochlorite that involves a solid-state process, and results in either βIII-CoOOH or β′III-CoOOH oxihydroxides, depending on the presence or absence of alkaline ions in the reaction medium, respectively;[5] (2) direct precipitation from a cobalt salt under oxygen pressure in alkaline conditions that leads to monolithic β-CoOOH;[6] and (3) hydrothermal oxidation in KOH medium under an oxygen pressure of 20 bar that occurs in a two-step mechanism, and results in the formation of mosaic CoOOH.[6]

Regarding the dry oxidation of cobalt hydroxide, using either pure oxygen or air as oxidizing agent, it was found that βII-$Co(OH)_2$ rapidly evolves into βIII-CoOOH, Co_2O_3, or Co_3O_4 depending on the reaction temperature. For instance, the βIII-CoOOH phase could be obtained as a single phase under oxygen flow at temperatures lower than 85 °C.[8−10]

With respect to γIII-CoOOH the synthesis is more complicated, and to our knowledge, only a ceramic

* To whom correspondence should be addressed. E-mail: fanny.barde@sc.u-picardie.fr.
† Université de Picardie Jules Verne.
‡ Institut de la Ciència de Materials de Barcelona (CSIC).

(1) Armstrong, R. D.; Briggs, G. W. D.; Charles, E. A. *J. Appl. Electrochem*. **1988**, *18*, 215−219.
(2) Delmas, C.; Faure, C.; Borthomieu, Y. *Mater. Sci. Eng.* **1992**, *B13*, 89−96.
(3) Folquer, M. E.; Vilche, J. R.; Arvía, A. J. **1984**, 143−148.
(4) Guerlou-Demourgues, L. Sur des nouveaux hydroxydes et oxyhydroxydes de nickel substitués au fer et au manganèse pour batteries nickel−cadmium ou nickel-hydrure métallique. Thesis, University of Bordeaux I, 1994.
(5) Butel, M. Étude des nouveaux oxyhydroxydes de cobalt pouvant être utilisés comme additif conducteur électronique ajoutés à l'hydroxyde de nickel dans les accumulateurs nickel/cadmium et nickel/métal hydrure. Thesis, University of Bordeaux I, 1998.
(6) Pralong, V.; Delahaye-Vidal, A.; Beaudoin, B.; Gérand, B.; Tarascon, J. M. *J. Mater. Chem*. **1999**, *9*, 955−960.
(7) Oshitani M.; Sasaki, Y.; Takashima, K. *J. Power Sources* **1984**, *12*, 219.
(8) Figlarz, M.; Guenot, J.; Fievet-Vincent, F. *J. Mater. Sci.* **1976**, *11*, 2267−2270.

10.1021/cm030054i CCC: $27.50
Published on Web 12/23/2003

process was reported up to now.[11,12] It consists, as demonstrated by Delmas' group, of an oxidizing hydrolysis of a ceramic precursor M_xCoO_2 (M = Na, K) that leads to γIII-CoOOH having a cobalt average oxidation state of 3.45.

In this paper we show that, through the use of ozone as oxidizing agent, γIII-like phases can be obtained at room temperature using either β or α $Co(OH)_2$ phases as precursors. For reasons of clarity, the paper will be organized as follows. We will first review the αII-$Co(OH)_2$ and βII-$Co(OH)_2$ phases synthesis methods and characteristics, and then describe the ex situ monitoring of the α and β oxidation process using ozone as compared to NaClO as oxidizing agent. Finally, for comparison purposes, the electrochemical behavior and the performances of the resulting oxidized phases will be presented and compared with those of the γIII-CoOOH phase obtained via the ceramic process.

Experimental Section

Syntheses of the Starting and Reference Materials. The **αII-$Co(OH)_2$** phase was obtained according to reference 13. A 20-mL aliquot of a 0.5 M solution of cobalt acetate was added to 100 mL of 0.5 M ammonia solution containing dissolved NaCl salt. An olive-color precipitate rapidly appeared at room temperature under strong stirring conditions. After the precipitate was washed and quick-dried, it was identified as αII-$Co(OH)_2$.

For **β-$Co(OH)_2$**, we used a commercial hydroxide precursor produced by UMICORE (Belgium) in the form of a pink powder.

For comparison purposes, γ-CoOOH (noted γ-$CoOOH_{ceramic}$) was also prepared according to published methods.[11] The first step consists of obtaining a ceramic precursor $K_{0.5}CoO_2$, by heating at 450 °C a Co_3O_4/KOH mixture under oxygen pressure. This compound is then oxidized by NaClO/KOH solution to form the γIII-CoOOH phase.

Ozonation System. An ozone generator, BMT 803, based on an electric arcing of a pure oxygen flow (quality 99.999%) was used to produce ozone. A flowmeter regulates the oxygen flow (0.2 NL/min) and therefore the amount of ozone produced (around 8 g/h). Then, the gas goes through a dry or moist atmosphere, before entering a vertical reactor, which simply consists of a glass tube separated in two parts in order to easily place and remove the sample. Roughly in the middle of the bottom part of the tube, there is a sinter where the hydroxide or a solid mixture KOH−hydroxide is placed. At the exit of the reactor the nonreactive ozone is destroyed by a reducing solution containing sodium thiosulfate and potassium iodide acting as an indicator. For safety reasons, Teflon ribbon was preferred to silicone paste to ensure hermetic sealing.

The experiments reported in this paper were conducted at room temperature as follows. A 1−1.5 g portion of powder was generally used, consisting of the hydroxide phase alone, unless otherwise specified. In some cases, a mixture of $Co(OH)_2$ and ground KOH pellets was used because, as described later, the presence of alkaline cations is needed for the formation of some phases. The potassium hydroxide can be added either at the beginning of the reaction or during the reaction. The latter protocol will be referred to as a two-step process consisting of (1) the oxidation of the cobalt hydroxide alone and (2) the reaction of the hydroxide in conjunction with KOH. We experienced that the moment at which KOH was added and its amount were very critical in the completion of reactions and the obtaining of single phases, as will be presented later.

Physical Characterization. Samples withdrawn at different stages of ozonation were investigated by XRD, TEM, EDS, TGA, and DSC. Their phase composition was determined by X-ray powder diffraction (XRD) using a Bruker D8 apparatus with a Co anticathode (λ = 1.79026 Å) in a θ/θ geometry with a position-sensitive detector (PSD) as counter. X-ray diffraction as a function of temperature was performed using the same diffractometer, as it was equipped with an HTK 1200 Anton Paar oven. During these in situ experiments, diffractograms were collected every 20 °C and 100 °C once the temperature had stabilized at ±1 °C within the 30−310 °C and 400−800 °C temperature window ranges, respectively. The sodium and cobalt contents were analyzed by energy dispersive X-ray spectroscopy (EDS) using a Philips XL-30FEG scanning electron microscope (SEM). Transmission electron microscopy (TEM) observations were performed with a Philips CM12 to determine morphology and structural changes. Thermogravimetric analysis (TGA) measurements were conducted on a Mettler Toledo apparatus, under ambient air at the rate of 1 °C/min over a 25−800 °C range of temperatures. Dispersive scanning calorimetry (DSC) curves were registered on the same apparatus at a rate of 5 °C/min over a 25−500 °C temperature window. The average oxidation state of the metal element within the prepared phases was determined by iodometric titration, whereas the total amount of cobalt was dosed using an ethylene diamine tetraacetic acid (EDTA) solution. Typically, 100 mg of the sample was added to 1.5 g of potassium iodide, and the mixture was dissolved in an acetic buffer solution. Sodium thiosulfate solution was used to titrate the iodine produced during cobalt reduction. Then, an ammonia solution was added to the media and the complexometric titration was carried out with an EDTA solution in the presence of murexide as indicator. The analyses were duplicated on each sample.

Electrochemical tests were performed in a three-electrodes configuration, using an Hg/HgO electrode as reference and nickel as counter electrode. The positive electrode consisted of a mixture of the active material (i.e., the cobalt oxihydroxide to be tested) with MCMB 25−28 carbon in a 1:5 ratio. Potassium hydroxide (5N) was used as electrolyte. Galvanostatic measurements were registered on an Arbin system at discharge rates of C/20.

Results

A. Ozonation of βII-$Co(OH)_2$ Hydroxide. βII-$Co(OH)_2$ presents a hexagonal structure similar to that of βII-$Ni(OH)_2$ with $P\bar{3}m1$ space group and slightly different cell parameters: a = 3.17 Å and c = 4.64 Å for the former and a = 3.12 Å and c = 4.61 Å for the latter. This hydroxide has a lamellar structure consisting of a stacking of CoO_2 layers arranged along the c axis. Commercial $Co(OH)_2$ precursor, from UMICORE, contains thin hexagonal platelets with an average diameter of 1500 Å and a thickness of 300 Å, as determined by TEM. They are monolithic as deduced from the presence of only well-defined spots on the selected area electron diffraction (SAED) picture together with the presence of Bragg fringes on the bright field image (Figure 1).

Two different synthesis protocols were carried out to conduct oxidation of the βII-$Co(OH)_2$ phase consisting of adding KOH in the course of reaction (1) or right at

(9) Tournemolle, J.-N. Étude de l'oxidation de Co(OH)2 en CoOOH et de la décomposition de CoOOH en Co3O4. Évolution de l'habitus et de la texture des particules solides en cours de réaction. Thesis, University of Paris VI, 1972.

(10) Soubirous, R. Déshydratation, oxidation et réduction de l'hydroxyde de cobalt II dans des conditions hydrothermales: étude des phases solides et des mécanismes de réaction. Thesis, University of Paris, 1970.

(11) Butel, M.; Gautier, L.; Delmas, C. *Solid State Ionics* **1999**, *122*, 271−284.

(12) Gautier, L. Influence du cobalt sur le comportement de l'hydroxyde de nickel dans les batteries alcalines: du substituant au collecteur de charges. Thesis, University of Bordeaux I, 1995.

(13) Rajamathi, M.; Kamath, P. V.; Seshadri, R. *Mater. Res. Bull.* **2000**, *35*, 271−278.

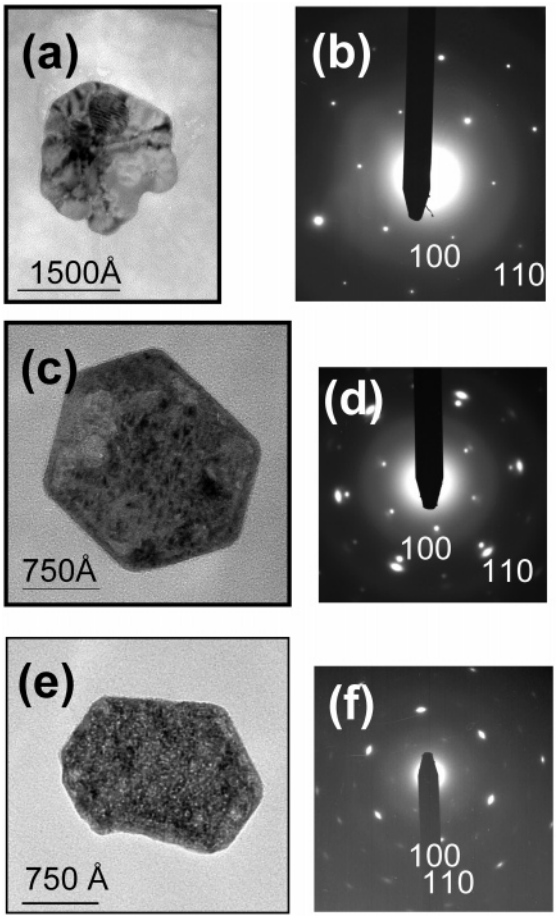

Figure 1. TEM images of (a) platelet of the initial βII-$Co(OH)_2$ product; (b) SAED on the particle represented on (a); (c) platelet from a sample removed after 4 h of reaction under dry ozone without KOH; (d) SAED on the particle represented on (c); (e) platelet from a sample removed after 69 h of reaction under dry ozone without KOH; and (f) SAED on the particle represented on (e).

the beginning (2). When KOH was added, we experienced that its amount and the presence of moisture were very critical in the completion of reactions and the obtaining of single phases, as observed for the $Ni(OH)_2$ system.[14]

(1) βII cobalt hydroxide was first placed alone in the reactor, and the ozone flow was turned on. Figure 2 shows the evolution of X-ray diffraction of samples removed at different stages of the reaction. With increasing reaction times, the X-ray diagrams indicate the coexistence of both phases βII-$Co(OH)_2$ and βIII-CoOOH with a vanishing of the peaks corresponding to βII at the expense of those of the βIII phase that are becoming unique after 69 h of ozone treatment. The noticeable shift of the Bragg peaks within the 20−30° scattering angle range clearly reveals a shortening of the *c* parameter from 4.64 to 4.40 Å, and is indicative of the transformation of the hydroxide into oxihydroxide. The obtained βIII-CoOOH, noted βIII_{1step}, can be indexed on the basis of a rhombohedral unit cell ($R\bar{3}m$ space group) with the cell parameters $a = 2.85$ Å, $c = 13.15$ Å.

Pursuing the ozonation for several hours in the presence of potassium hydroxide did enable the synthesis of β'III-CoOOH phase, denoted hereafter $\beta' III_{2steps}$ (Figure 2), in which the cobalt average oxidation degree was found to be 3.07 compared to only 3 for the βIII_{1step} phase. The main difference between βIII and β'III oxihydroxides lies on the fact they present different oxidation degrees.

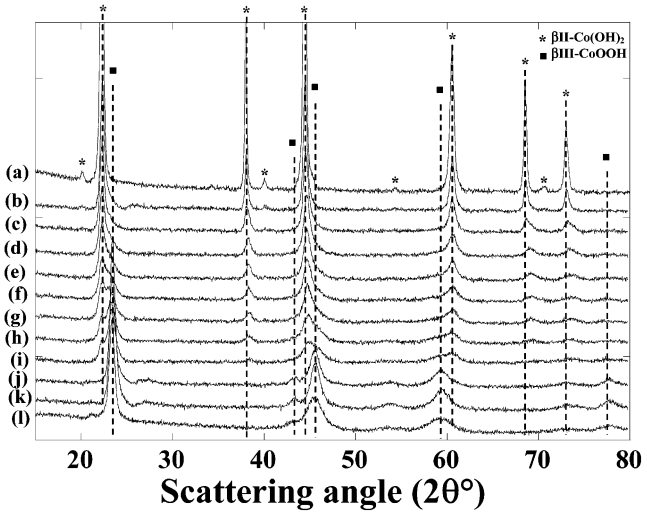

Figure 2. X-ray diffraction patterns of intermediate samples removed during the ozonation of βII-$Co(OH)_2$ alone: (a) initial βII-$Co(OH)_2$ phase; (b) after 30 min under dry ozone atmosphere; (c) after 1 h; (d) after 1 h 30 min; (e) after 2 h; (f) after 3 h; (g) after 4 h; (h) after 22 h; (i) after 24 h 30 min; (j) after 42 h; (k) after 69 h; and (l) sample obtained after ozone treatment of (k) for 4 more hours in the presence of KOH.

Finally, the microscopic images and SAED patterns (Figure 1) that show the transformation of the monolithic βII-$Co(OH)_2$ particles (thin spots) into mosaic βIII-CoOOH particles (broad arcs) upon ozonation, unambiguously prove the pseudomorphous and topotactical character of the ozonation process.

(2) The main difference with the former experimental protocol is that potassium hydroxide was added from the beginning of the ozonation. Under such conditions, with ozone atmosphere, we observed the direct formation of the nonstoichiometric β'III cobalt oxihydroxide (noted $\beta' III_{1step}$) with an oxidation degree of 3.07 (Figure 3). However, this phase had lower crystallinity than the β'III oxihydroxides obtained according to protocol (1) i.e., $\beta' III_{2steps}$.

The highest cobalt oxidation state that could be reached was 3.07, whatever synthesis protocol used. This value suggests, according to the literature,[4−6] the presence of 0.7 Co(IV) cations, and so electronic conductivity should be expected. Therefore, the βII-$Co(OH)_2$ phase never evolves into γIII-CoOOH even in the presence of alkaline ions. This is in total contrast with the nickel case where, upon oxidation, βII-$Ni(OH)_2$ easily transforms into γIII-NiOOH.[14,15]

B. Ozonation of the αII−Co(OH)$_2$ Hydroxide. αII-$Co(OH)_2$ was prepared, according to the procedure described in the literature,[13] by a NaCl-assisted precipitation of cobalt chloride in aqueous ammonia medium, which is recognized to lead to the presence of Cl^- species between the CoO_2 sheets. Chemical analysis

(14) Bardé, F. et al. Manuscript in preparation to be submitted for publication.

(15) Sac-Epée, N.; Palacin, M. R.; Beaudoin, B.; Delahaye-Vidal, A.; Jamin, T.; Chabre, Y.; Tarascon, J. M. *J. Electrochem. Soc.* **1996**, *144*, 3896−3907.

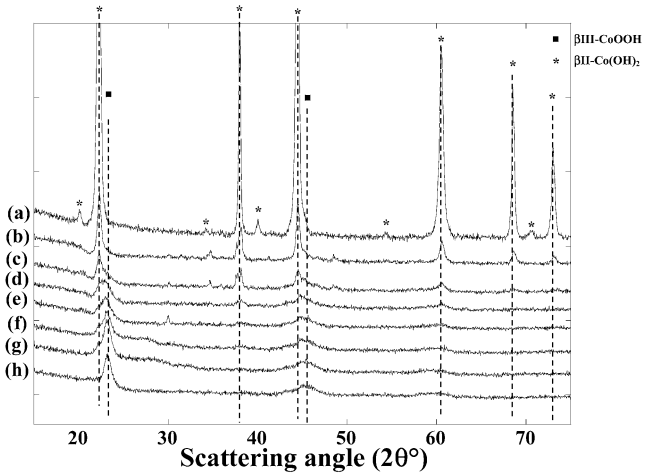

Figure 3. X-ray diffraction patterns of intermediate samples removed during the ozonation of βII-$Co(OH)_2$ in the presence of potassium hydroxide: (a) initial βII-$Co(OH)_2$ phase; (b) after 30 min under moist ozone atmosphere; (c) afer 1 h; (d) after 2 h; (e) after 4 h; (f) after 5 h 30 min; (g) after 18 h 30 min; and (h) after 26 h.

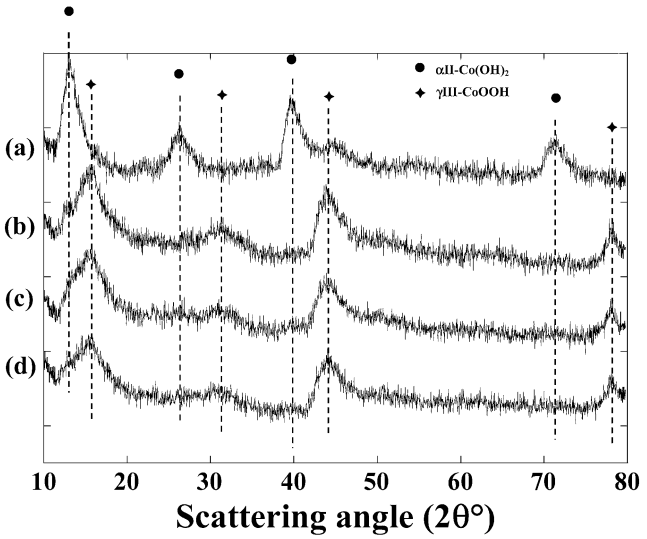

Figure 4. X-ray diffraction patterns of samples removed during the ozonation of αII-$Co(OH)_2$: (a) initial αII-$Co(OH)_2$ phase; (b) after 30 min under dry ozone atmosphere; (c) after 1 h; and (d) after 4 h.

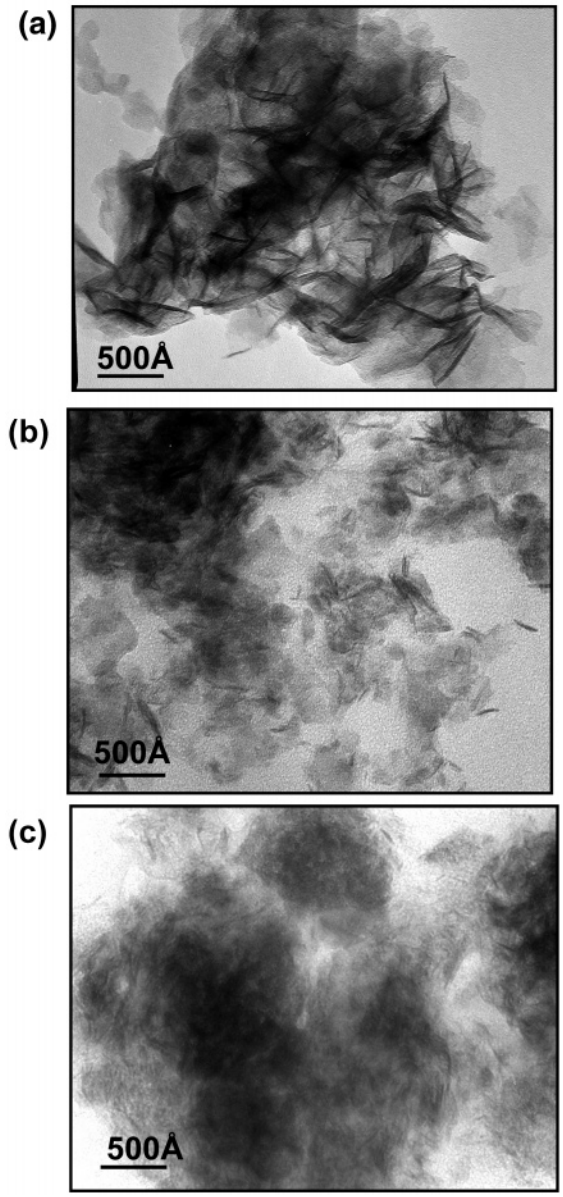

Figure 5. TEM photos of cobalt hydroxides and oxihydroxides (a) αII-$Co(OH)_2$; (b) γIII_{O3}; and (c) γIII_{NaClO}.

and TGA measurement performed on the precipitated α powder result in its exact formula: $Na_{0.08}Co(OH)_{1.83}(Cl)_{0.25}\cdot 0.70H_2O$. The X-ray diffraction pattern (Figure 4a) of this α-phase precursor exhibits broad Bragg peaks denoting its poor crystallinity. Furthermore, some of the peaks are asymmetric, indicating the turbostratic character of the material. This results from a disorder of the CoO_2 layers (separated by water molecules and anions) along the *c* axis (c = 7.84 Å) while the *a* lattice parameter remains around 3.09 Å. αII-$Co(OH)_2$ powders appear as aggregates of very thin tangled films without any particular morphology (Figure 5a).

The instability of the alpha cobalt phase in basic media was put forward as the origin of the difficulty encountered for a long time in its preparation. To confirm this fact, we mixed αII-$Co(OH)_2$ with potassium hydroxide, and noted an instantaneous evolution of αII into βII as deduced from the X-ray diffraction pattern of the resulting mixture that exhibits the coexistence of two sets of Bragg peaks with, in addition, extra peaks corresponding to KCl salt. Such a rapid evolution of α into β is most likely nested in the formation of KCl that results from the removal of the Cl^- interlayer anions leading to a drastic decrease in the *c* parameter. The same test conducted with sodium hydroxide led to similar results with namely the rapid formation of αII into βII in conjunction with the appearance of NaCl salt. In light of such findings, we only pursued the ozonation of αII-$Co(OH)_2$ in absence of potassium hydroxide.

Aliquots of 500 mg of αII-$Co(OH)_2$ were treated under dry ozone atmosphere for various times, and were subsequently recovered during the course of the reaction for X-ray investigations. Only the most relevant X-ray diffraction patterns are reported on Figure 4. We observed the complete oxidation of αII-$Co(OH)_2$ into γIII-CoOOH after 4 h. Patterns 4b and 4c show the coexistence of the two phases. The *c* parameter evolves from 7.84 Å for the precursor phase to 6.78 Å for the fully oxidized phase, denoted γIII_{O3}, characterized by an amorphous diffraction pattern reminiscent of its poor

Table 1. Comparison of *d* Values Measured from X-ray Diffractograms for γIII-CoOOH Obtained by Ceramic Route or Soft Chemistry

(*hkl*)	*d* (Å) observed $\gamma III_{ceramic}$	*d* (Å) observed $\gamma III_{O3/NaClO}$ (±0.1 Å)
(003)	6.79	6.7
(006)	3.40	3.4
(101)	2.43	2.4
(110)	1.41	1.4
(113)	1.39	

crystallinity (Figure 4d). The average *d* (Å) distances deduced from an analysis of the peak positions observed on the γIII_{O3} diffractogramm are reported in Table 1 and compared to those obtained from the X-ray pattern of γIII-CoOOH$_{ceramic}$ obtained by the ceramic process. Within the accuracy of the measurements, the results coincide.

From TEM studies (Figure 5b), no textural change during ozonation was noted, and the oxidized γIII_{O3} phase consisted of aggregates of very thin tangled films as did the initial α phase.

Finally, the average cobalt oxidation state within the γIII_{O3} phase was determined as being equal to 3.16, suggesting that 0.16 cobalt cations are in the IV oxidation state. From this result combined with EDS and TGA analyses performed on the sample, the formula $Na_{0.07}Cl_{0.04}H_{0.82}CoO_2 \cdot 0.7H_2O$ was deduced for γIII_{O3}. Interestingly, the sodium content is almost the same as that observed for the initial α phase, whereas the chloride content has noticeably decreased, suggesting that, upon ozonation, part of interlayer species (Cl^- anions) are expelled.

C. Synthesis of γIII-CoOOH by Solution Means. This last approach, widely used for the oxidation of β nickel phases, consists of adding 1 g of αII-Co(OH)$_2$ to 100 mL water and treating the resulting mixture with sodium hypochlorite at 50 °C during 4 h. Then, the product is copiously washed with water and dried for 15 h at 55 °C. The diffractogram of the obtained phase, denoted γIII_{NaClO}, turned out to be quite similar to that of γIII_{O3}, with both phases having the same *d* spacing (Table 1). Transmission electron microscopy studies (Figure 5c) further confirmed the similarity between γIII_{NaClO} and γIII_{O3} from both a morphologic and structural point of view.

Surprisingly, despite these similarities, we noted differences in the cobalt oxidation state, composition, and thermal stability of both phases. For instance, an average cobalt oxidation state of 3.27 was measured for γIII_{NaClO} as compared to 3.16 for γIII_{O3}. In addition, γIII_{NaClO} was found to contain no chloride but 33% of sodium within its structure, whereas 4% chloride and 7% sodium were found for γIII_{O3} resulting in the formula: $Na_{0.33}H_{0.42}CoO_2 \cdot 0.8H_2O$ and $Na_{0.07}Cl_{0.04}H_{0.82}CoO_2 \cdot 0.7H_2O$, respectively. Water content was deduced from the TGA curves presented later.

D. Comparison Between the Different Cobalt Oxidized Phases. *D.1 Thermal Study.* Figure 6a presents TGA of the starting phases αII-Co(OH)$_2$ and βII-Co(OH)$_2$ and of the different β-type cobalt oxihydroxides obtained by ozonation.

Typically, at 200 °C a drastic weight loss of 15% (Figure 6a) is observed during the heating of βII-Co(OH)$_2$, whereas for αII-Co(OH)$_2$ the weight loss reaches 27% and takes place in three steps as delimited

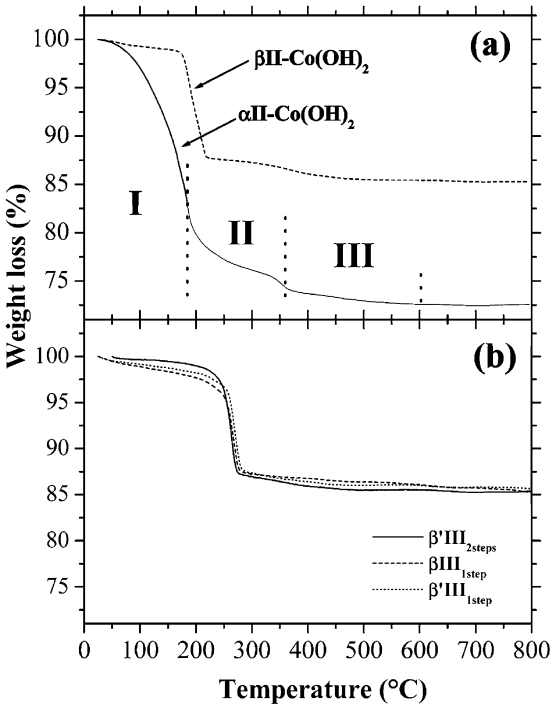

Figure 6. TGA of cobalt hydroxides and oxihydroxides (a) αII-Co(OH)$_2$ and βII-Co(OH)$_2$; and (b) β′III$_{2steps}$, βIII$_{1step}$, and β′III$_{1step}$.

by the zones noted I, II, and III on the graph. The absorbed and intercalated species are lost in a single broad step (domain I) in the range of 25−200 °C. The domain II ranging from 200 to 350 °C is associated with the loss of water produced by dehydroxylation of the hydroxide layers combined with the loss of a part of the anionic species (Cl^-). Finally, the third domain (noted III) ending at 500 °C could be attributed to the loss of adsorbed ions. These results are in good agreement with previous literature reports.[13] For βII-Co(OH)$_2$, the hydroxyl groups' departure together with the conversion into Co_3O_4 that follows are responsible for the total weight loss. The water content in αII-Co(OH)$_2$ was calculated from the weight loss between 25 and 150 °C, and was estimated as being equal to 0.7.

The three β cobalt oxihydroxides (β′III$_{2steps}$, βIII$_{1step}$, and β′III$_{1step}$) present a similar behavior upon thermal treatment (Figure 6b). As determined by XRD measurements on the TGA recovered samples, the hydroxyl groups' departure from CoOOH leading to the Co_3O_4 phase are at the origin of the observed weight loss.

For the new γIII_{NaClO} and γIII_{O3} cobalt oxihydroxides, TGA measurements were recorded at a heating rate slower (1 °C/min) than the DSC rate (5 °C/min) to ensure good separation of the different thermal phenomena. These experiments allowed determination of the water content of the samples, which turned out to be 0.7 and 0.8 for γIII_{O3} and γIII_{NaClO}, respectively.

Figure 7a represents the TGA and DSC curves for γIII_{O3}. A 25% weight loss occurring in two steps can be noted. The first step corresponds to the departure of the interslab water molecules, and the second one is due to the loss of hydroxyl also in the form of H_2O. The trace shows two distinct endothermic peaks that are directly correlated to each of the above phenomena, in addition to an exothermic peak appearing around 250 °C that could be assigned to the crystallization of Co_3O_4.

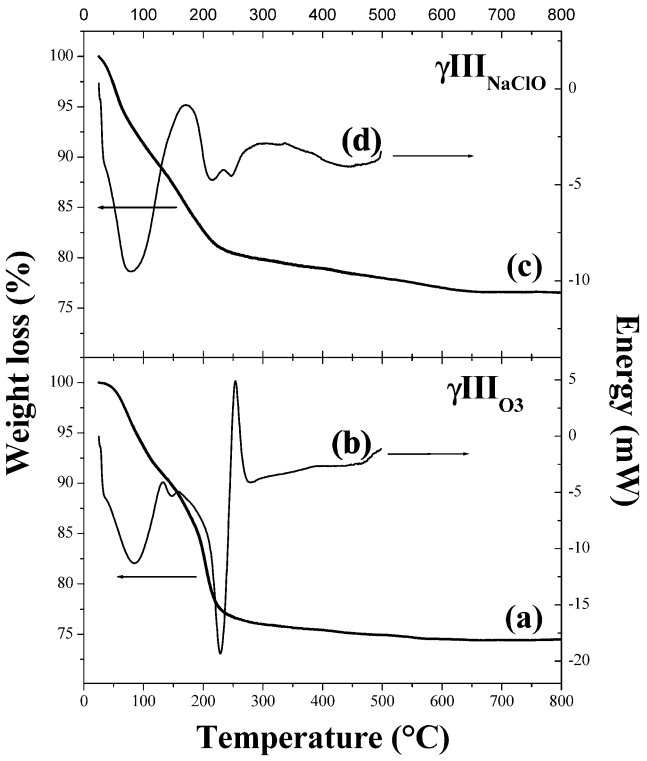

Figure 7. (a) TGA and DSC of γIII_{O3}, and (b) TGA and DSC of γIII_{NaClO}.

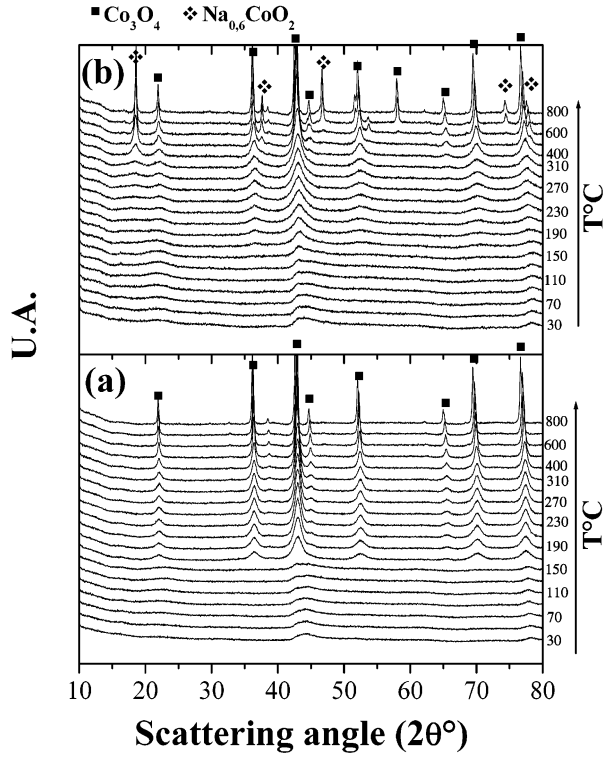

Figure 8. In situ X-ray diffraction study as a function of temperature for γIII_{O3} (a) and γIII_{NaClO} (b).

In situ X-ray diffraction with temperature (Figure 8a) is in good agreement with these results. The initial γIII_{O3} poor diffractogram begins to show Co_3O_4 peaks at about 160 °C. Then, there is a coarsening of the Co_3O_4 particles with increasing temperature, and at 800 °C the X-ray powder pattern is characteristic of pure well-crystallized Co_3O_4.

Regarding the γIII_{NaClO} (Figure 7b), the interpretation is less straightforward because the TGA curve presents two distinct slopes. The first well-defined endothermic peak is correlated to the first part of the TGA curve, and is assigned to water loss in the sample and heat decomposition of CoOOH. The latter endothermic phenomenon identified on both TGA and DSC experiences begins at 200 °C and goes on up to at least 650 °C. It consists of an endothermic process. The evolution of the in situ X-ray diffraction patterns as a function of temperature (Figure 8b) indicates a slow transformation of CoOOH into Co_3O_4. At 310 °C, two sets of broad extra peaks appear and sharpen with increasing temperature: one set perfectly corresponds to Co_3O_4 whereas the second set of Bragg peaks falls at positions close to those expected for $Na_{0.6}CoO_2$. The growth of such a phase is consistent with the 33% sodium content within the starting sample. The slight deviation may arise from nonstoichiometric phases prone to exist with the $Na_{0.6}CoO_2$ system.[16]

In summary, the main difference observed between the γIII-CoOOH samples produced either upon ozonation or by oxidation in solution is their thermal behavior. Upon heating, γIII_{O3} drastically transforms into pure Co_3O_4 around 160 °C, whereas γIII_{NaClO} leads to the coexistence of two phases: Co_3O_4 and Na_xCoO_2. Such difference is simply nested in the difference between the sodium contents within the precursors.

D.2 Chemical Stability of γIII-CoOOH Phases. To test the stability of γIII_{O3} phase in concentrated KOH medium, 200 mg of γIII_{O3} was placed in a 5 N potassium hydroxide solution during 3 h, and the resulting product was then centrifuged, washed several times in water, and dried at 55 °C prior to being characterized for phase purity and cobalt oxidation state. XRD, not shown here, indicates that the sample transforms into a β-like phase. Solely on the basis of the cobalt oxidation state (3.08), as determined by titration, this β phase is more likely of β'III-CoOOH-type nature. This experiment further highlights the great instability of γIII_{O3} in concentrated basic medium, hence the difficulty to preserve the γIII phase as a coating in batteries.

For comparison purposes, an identical experiment was performed on γIII_{NaClO}. After analysis of the X-ray diffraction pattern, no evidence of transformation upon aging was found, neither did the cobalt oxidation state change, as it remained equal to 3.27.

Thus the direct evidence for the greater chemical stability of γIII_{NaClO}, as compared to γIII_{O3}, in KOH media was unambiguously proved.

D.3 Electrochemical Tests. The electrochemical performances of the synthesized β and γ phases (Figure 9) exhibit the discharge of each phase oxidized by ozonation or by NaClO, namely $\beta' III_{1step}$, $\beta' III_{2steps}$, γIII_{O3}, and γIII_{NaClO}. For comparison, we also reported the electrochemical curve of $\gamma III_{ceramic}$ (e.g., $K_{0.5}CoO_2$) collected under identical experimental conditions. More specifically, we explored the potential domain ranging from −0.5 to 0.2 V versus Hg/HgO, which is reported in the literature as the potential window over which the reduction of tetravalent ions Co^{4+} into trivalent Co^{3+} occurs. A pseudo plateau at 0 and 0.1 V versus Hg/HgO

(16) Delmas, C.; Braconnier, J.; Maazaz, A.; Hagenmuller, P. *Rev. Chim. Miner.* **1982**, *19*, 343.

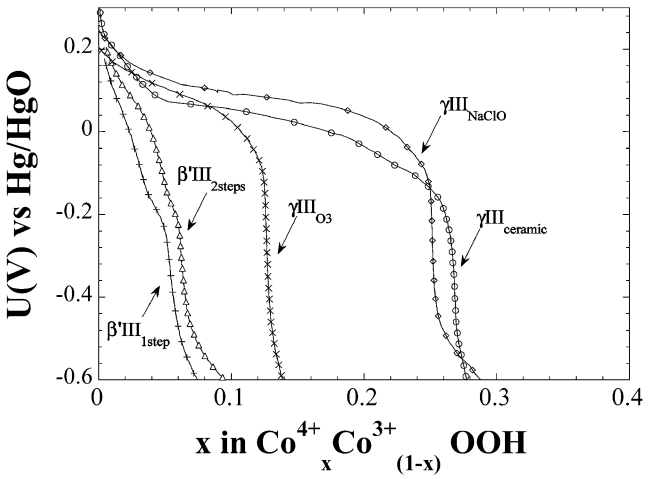

Figure 9. Electrochemical performances of different cobalt oxihydroxides prepared by either soft chemistry or ceramic route.

was observed for the γIII-CoOOH and β′III-CoOOH phases, respectively (Figure 9). The amplitude of this plateau (e.g., number of electrons exchanged, NEE) is highly dependent on the phase. The obtained NEE values were compared to the average cobalt oxidation state measured on each phase (Table 2), and a direct correlation between both sets of values was noted. This fact indicates that all Co(IV) present in the structure participated in the electrochemical reduction.

Along that line it is totally expected that the βIII_{1step} phase, which does not contain any tetravalent cobalt as experimentally measured, has no electrochemical signature in the studied domain. Both nonstoichiometric $\beta'III_{2steps}$ and $\beta'III_{1step}$ obtained by ozone exchange 0.07 electrons, again in agreement with the cobalt oxidation state of 3.07 measured by iodometric titration. With a NEE = 0.13, γIII_{O3} has an intermediate behavior lying between that of γ ($\gamma III_{ceramic}$, γIII_{NaClO}) and that of β′III (β′III_{1step}, β′III_{2steps}) phases. Finally, compared to $\gamma III_{ceramic}$, γIII_{NaClO} presents the same attractive electrochemical signature over the explored potential window with the merit of being prepared at low temperature. We should be very careful not to overinterpret the discharge potential difference between the $\gamma III_{ceramic}$ and the γIII_{NaClO} samples, which is simply the result of particle size difference. With the particles being larger for the $\gamma III_{ceramic}$, we expect a lower potential under similar cycling conditions as experimentally observed.

Discussion

We have shown that different β-type CoOOH phases can be obtained by treatment of βII-$Co(OH)_2$ with ozone. They all present the same structure, but their major difference lies in their cobalt average oxidation state (e.g., amount of Co(IV)) and therefore in their electrochemical behavior. This is the reason both $\beta'III_{2steps}$ and $\beta'III_{1step}$ have a 0.07 electron discharge capacity instead of 0.00 for the βIII_{1step}, which has only a III+ oxidation state. In light of previous reports[5,6] that have shown that the conductivity aspect of these phases scales with the amount of Co(IV), and is the highest for the greatest amount of Co(IV), the nonstoichiometric $\beta'III_{2steps}$ or $\beta'III_{1step}$ could present an interest when coated on $Ni(OH)_2$ particles as they are proved to exhibit a greater conductivity.

Concerning the γ-type CoOOH phase, we succeeded in preparing two new phases using exclusively soft chemistry. Figure 10 summarizes the two exploited synthesis routes to oxidize αII-$Co(OH)_2$. Regarding the mechanism paths, considering there are only traces of chlorides in the final γIII-CoOOH phases while Cl^- is abundant in the starting material, it seems logical to propose that the oxidation process involves the expulsion of Cl^- issued from the α precursor. Simultaneously, there is a departure of H^+ from the structure implying

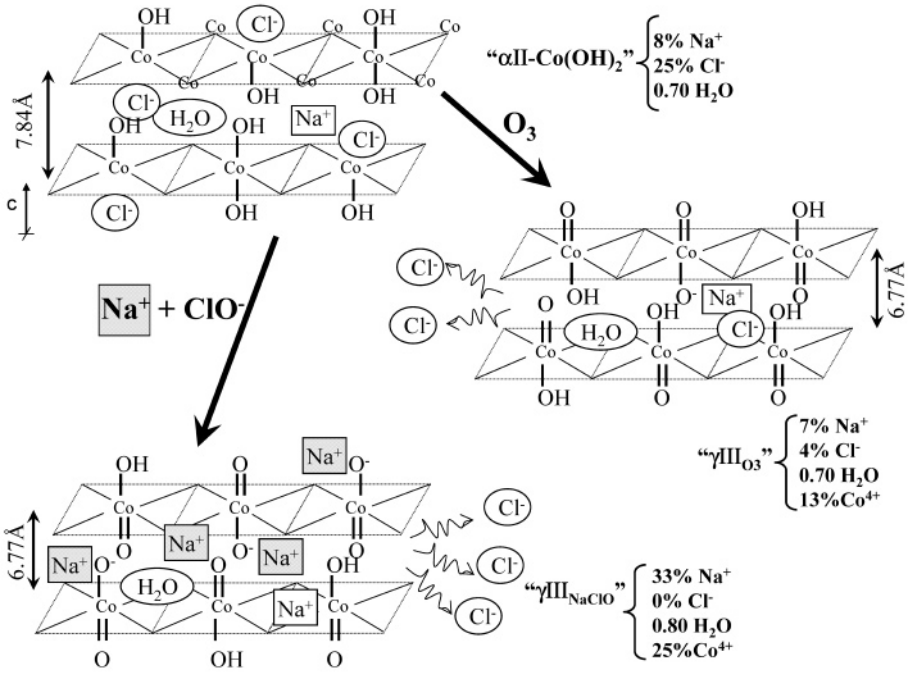

Figure 10. Recapitulative diagram of oxidation mechanisms leading to either γIII_{O3} or γIII_{NaClO} products starting from αII-$Co(OH)_2$.

Table 2. Oxidation Degrees and Electrochemical Performances (NEE) of the Different Cobalt Oxihydroxides

	βIII_{1step}	$\beta' III_{2steps}$	$\beta' III_{1step}$	γIII_{O3}	γIII_{NaClO}	$\gamma III_{ceramic}$
oxidation degree	2.95−2.99	3.05−3.08	3.05−3.08	3.13−3.16	3.26−3.30	3.35−3.40
x in $Co^{4+}_x\ Co^{3+}_{(1-x)}OOH_{(1-x)}$[a] (or NEE)	0.00	0.07	0.06	0.13	0.25	0.28

[a] U (volts) > −0.4 V vs Hg/HgO.

the formation of Co═O bounds entailing an increase in the cobalt oxidation state. The major difference between the two oxidation routes studied is nested in the presence of Na^+ during the NaClO oxidation as compared to the ozonation process. Indeed, the sodium atomic content was estimated at 33% in γIII_{NaClO} against only 7% in γIII_{O3}. This last value coincides exactly with the initial sodium content found in αII-$Co(OH)_2$ as expected. Besides, interestingly, in the γIII_{NaClO} phase Na^+ and Co^{4+} contents seem to be linked. Using NaClO in excess to ensure a complete oxidation, the maximum sodium content that we can reach in γIII_{NaClO} is 33%. This is less than what can be achieved for the ceramic sample. This difference between Na contents is compensated by the presence of more protons in γIII_{NaClO} as deduced by means of TGA, thus, explaining the poor crystallinity of γIII_{NaClO} due to the poor screening role of H^+ as compared to that of Na^+ between the two repulsive CoO_2 slabs. Nevertheless, the electrochemical activity of both products γIII_{NaClO} and $\gamma III_{ceramic}$ is quite similar. In light of the above results combined with those from Delmas' group,[5,11,12] it becomes apparent that γIII-CoOOH can be obtained only by starting from a precursor already presenting a large interslab space (the αII-$Co(OH)_2$ phase or the Na_xCoO_2 precursor, respectively). This behavior contrasts with that of γ nickel oxihydroxides, which can be obtained easily by starting from βII-$Ni(OH)_2$, although the difference of the interlayer space between the nickel γ and β phases is of the same order as the spacing between the γ and β cobalt phases. Such a difference is most likely nested in the iono-covalence of the M−O bonding as discussed by Delmas' group.[16]

Conclusion

We have explored two different syntheses routes to prepare either β- or γ-type cobalt oxihydroxides. Among all the oxidized phases we prepared, γIII_{NaClO} turned out to be the most attractive for electrochemical applications due to the largest amount of Co^{4+} (25%) resulting in a higher capacity combined with a better conductivity. Furthermore, another positive aspect of γIII_{NaClO} is that it does not evolve upon aging, at least up to a few days.

Such a chemical stability reported for γIII_{NaClO} strengthens a possible utilization of this phase as a coating on nickel hydroxide. However, this is not an easy task as we presently experienced through our attempts to homogeneously deposit αII-$Co(OH)_2$ on $Ni(OH)_2$ particles.

Acknowledgment. We give special thanks to M. Nelson, V. Pralong, and the Gillette's research team for helpful discussions.

CM030054I